Canadian Journal of
Forest Research

OPEN ACCESS | Article

Harmonizing multi-temporal airborne laser scanning point clouds to derive periodic annual height increments in temperate mixedwood forests

José Riofrío[a], **Joanne C. White**[b], **Piotr Tompalski**[b], **Nicholas C. Coops**[a], **and Michael A. Wulder**[b]

[a]Integrated Remote Sensing Studio, Department of Forest Resources Management, University of British Columbia, 2424 Main Mall, Vancouver, BC V6T 1Z4, Canada; [b]Canadian Forest Service (Pacific Forestry Centre), Natural Resources Canada, 506 West Burnside Road, Victoria, BC V8Z 1M5, Canada

Corresponding author: **José Riofrío** (email: jriofrio@mail.ubc.ca)

Abstract

When combining multi-temporal airborne laser scanning (ALS) data sets, forest height growth assessments can be compromised due to variations in ALS acquisitions. Herein, we demonstrate the importance of assessing and harmonizing the vertical alignment of multi-temporal ALS data sets used for height growth calculations. Using four ALS acquisitions (2005–2018) in a temperate mixedwood forest, we developed an ALS data harmonization approach and quantified the impact of the harmonization on derived height periodic annual increment (PAI), comparing the ALS-derived PAI to PAI derived from non-harmonized ALS data sets and field measurements. We found significant differences in PAI derived from harmonized and non-harmonized data, and these differences were greater for shorter growth intervals. Data harmonization resulted in a consistent PAI series that reduced uncertainties associated with the different ALS acquisitions. Although overall there was a strong relationship between field and ALS height measures ($R^2 \geq 0.88$), we found a weak relationship between the field- and ALS-derived PAI ($R^2 = 0.12$). We identified systematic errors in field-based tree height measures in plots with complex crowns, tall trees, and restricted visibility. We demonstrate the need for harmonizing multi-temporal ALS data sets for the generation of PAI and, likewise, highlight the need of carefully scrutinize field-measured heights and associated increments.

Key words: multi-temporal ALS, height increment, vertical alignment, data harmonization, temperate mixedwood forest

Résumé

Lors de la combinaison d'ensembles de données de balayage laser aéroporté (ALS) multitemporels, les évaluations de la croissance en hauteur des forêts peuvent être compromises en raison des variations dans les acquisitions de l'ALS. Nous démontrons ici l'importance d'évaluer et d'harmoniser l'alignement vertical des ensembles de données de l'ALS multitemporels utilisés pour les calculs de croissance en hauteur. En utilisant quatre acquisitions de l'ALS (2005–2018) dans une forêt mixte tempérée, nous avons développé une approche d'harmonisation des données de l'ALS et quantifié l'impact de l'harmonisation sur l'accroissement annuel périodique (PAI) dérivé de la hauteur, en comparant le PAI dérivé de l'ALS au PAI dérivé de jeux de données de L'ALS non harmonisés et de mesures sur le terrain. Nous avons trouvé des différences significatives dans le PAI dérivé des données harmonisées et non harmonisées, et ces différences étaient plus grandes pour les intervalles de croissance plus courts. L'harmonisation des données a permis d'obtenir une série de PAI cohérente qui a réduit les incertitudes associées aux différentes acquisitions de l'ALS. Dans l'ensemble, bien qu'il y ait une forte relation entre les mesures de hauteur sur le terrain et celles de l'ALS ($R^2 \geq 0{,}88$), nous avons trouvé une faible relation entre le PAI dérivé du terrain et celui dérivé de l'ALS ($R^2 = 0{,}12$). Nous avons identifié des erreurs systématiques dans les mesures de hauteur des arbres basées sur le terrain dans les parcelles avec des couronnes complexes, des arbres de grande taille et une visibilité limitée. Nous démontrons la nécessité d'harmoniser les ensembles de données de l'ALS multitemporels pour la génération du PAI et, de même, nous soulignons la nécessité d'examiner soigneusement les hauteurs mesurées sur le terrain et les accroissements associés. [Traduit par la Rédaction]

Mots-clés : ALS multitemporel, accroissement de hauteur, alignement vertical, harmonisation des données, forêt mixte tempérée

1. Introduction

Light Detection and Ranging (lidar) has revolutionized the capture of three-dimensional (3D) information pertaining to tree and forest structural attributes at varying spatial scales. Airborne laser scanning (ALS) technologies are now widely used to generate accurate estimates of vegetation height, cover, volume, biomass, and other aspects of forest productivity (White et al. 2016). In addition, the spatially explicit characterizations of vegetation structure and terrain derived from ALS data allows quantification and monitoring of a broad range of indicators in the context of sustainable forest management (Goodbody et al. 2021). From a forest management perspective, spatial data detailing changes in aggregated forest attributes such as timber volume or biomass per unit area provides key information for maintaining social, economic, and environmental values of forest (Wulder et al. 2008) and for understanding the stressors and disturbances affecting these forest ecosystems through time.

Knowledge of the future status of the forest resource is also critical for forest planning and sustainable forest management. Significant investments have been made by Canadian jurisdictions in growth and yield (G&Y) program; however, current growth models for some regions underrepresent more complex structural forest conditions, such as mixedwood, managed stands including mixed species plantations, and shelterwood silvicultural systems (Penner and Pitt 2019). Moreover, G&Y models often lack the flexibility to adapt to changing environmental conditions or new silvicultural practices (Sharma et al. 2008) and cannot readily integrate new data inputs, specifically wall-to-wall 3D measures of forest structure from ALS, as well as derived inventory attribute layers from Enhanced Forest Inventories (EFI) (Tompalski et al. 2021). As the acquisition of ALS is becoming more common, the availability of multi-temporal data sets is also increasing, allowing for the characterization of forest growth and dynamics. As summarized in McRoberts et al. (2014) and Tompalski et al. (2021), numerous studies have demonstrated the feasibility of characterizing change in forest attributes using multi-temporal ALS data. In most of these investigations, characteristics derived from height distributions of pulse returns (i.e., estimate the changes in canopy structure) were used for modelling area-based changes and for generating predictions of future forest stand conditions. This 3D forest information has the potential to improve G&Y projections in a number of ways: first, by providing direct, spatially explicit measurements of periodic height growth increments over large areas and across a range of forest and site conditions (Knapp et al. 2018; Zhao et al. 2018; Mauro et al. 2019; Tompalski et al. 2019); second, by enabling spatially explicit estimates of site quality (Tompalski et al. 2015; Socha et al. 2017; Noordermeer et al. 2020); and third, by allowing for the parameterization and development of ALS-driven growth simulators (Lamb et al. 2018; Tompalski et al. 2018).

The opportunities afforded by repeated ALS acquisitions also present certain challenges. ALS sensors and associated technologies have developed rapidly over the past three decades, enabling different acquisition parameters and resulting in greater point densities, wider scan angles, and different sensor types (e.g., single photon lidar, SPL). Moreover, data may be acquired with different levels of horizontal and vertical accuracy and may use different horizontal or vertical datums, as spatial reference systems also continue to evolve (Smith 2018). As a result, assessment of the planimetric and vertical correspondence between acquisitions is a key precursor to using these data to accurately characterize height growth. Pre-processing of ALS data sets (e.g., projection or datum transformation) may be required to ensure that changes detected in 3D point clouds represent real changes in the target of interest and do not result from differences in the data itself. Accounting for systematic or known differences in ALS acquisitions also ensures that associated errors or uncertainties are reduced in the resulting growth estimates.

Studies that have used multi-temporal ALS data to assess growth or change in forest attributes have adopted different approaches to pre-processing ALS acquisitions to account for the aforementioned differences between data acquisitions (Table 1). Yu et al. (2004) were the first to highlight the importance of co-registering and assessing differences in multi-temporal ALS point clouds when using these data for height growth estimation. However, approximately half of the studies we examined did not report assessing planimetric or vertical differences between the different ALS acquisitions used in their analyses nor did they report any form of pre-processing or harmonizing of data acquisitions. As presented in Table 1, among those studies that did assess and consider pre-processing, the majority selected one of their ALS acquisitions (and derived digital terrain model, DTM) as a reference for normalizing all other ALS acquisitions used in their study to heights above ground. Such approaches provide relative values that do not account for any systematic differences between acquisitions that may result from sensor characteristics or the accuracy with which the survey was conducted. Moreover, they assume that independent relief models for every acquisition represent a practically unchanged terrain for the analysed period (Økseter et al. 2015; Zhao et al. 2018; Dalponte et al. 2019; Tymińska-Czabańska et al. 2021). Only one study reported a detailed assessment and adjustment of ALS point clouds and used ground returns from all four acquisitions to generate a common DTM that was then used for normalization (Hopkinson et al. 2008). Two of the studies we reviewed focused on differences in the point density of the ALS acquisitions instead of assessing the planimetric or vertical differences between acquisitions. Zhao et al. (2018) considered both individual tree and area-based assessments of growth. To account for density differences among their four ALS acquisitions for their individual tree assessment, the authors applied a post hoc adjustment of individual tree heights based on an empirical correction, whereas they found no significant effect of density on their area-based assessment. Magnussen et al. (2015) thinned the point density of their ALS data to equalize the point clouds of their bi-temporal ALS data before generating a canopy height model (CHM) and deriving metrics. Previous studies have demonstrated that CHM-derived metrics are more sensitive to differences in ALS point density than metrics derived from the point cloud directly (Garcia et al. 2017).

Estimates of changes in forest attributes derived from repeat field measurements at field plot locations are fundamental data for assessing forest growth (Weiskittel et al. 2011). However, methods for measuring tree heights in the field are not immune to error, particularly in certain forest conditions that limit tree visibility, such as in stands with multi-layered vertical structures, large complex shaped tree crowns, or

Table 1. Summary of ALS pre-processing approaches in studies using multi-temporal ALS to assess height growth or change in forest attributes.

Study	ALS data	Approach	Comments
Yu et al. 2004	1998, 2000	Use the same DTM to normalize all acquisitions	ALS underestimated growth relative to field plots. DTM had a significant impact on ALS-derived estimates of growth, having both systematic and random errors. Compensated for this by using the same DTM to height normalize both acquisitions.
St-Onge and Vepakomma 2004	1998, 2003	Use same DTM to normalize all acquisitions	Assessed alignment of *x*, *y*, and *z*. No planimetric shifts in *x* or *y*. 22 cm difference in *z* of ground points. Followed the approach of Yu et al. (2004) and used 2003 DTM to height normalize of 1998 point clouds.
Næsset and Gobakken 2005	1999, 2001	Use same DTM to normalize all acquisitions	Used data from 2001 to normalize both acquisitions.
Hopkinson et al. 2008	2000, 2002, 2004, 2005	Combine ground returns from all acquisitions	Plantation forests. Used road surfaces to assess and adjust raw point clouds to conform to 2000 ALS data. Ground returns from all acquisitions were combined, filtered, and interpolated to generate a DTM that was used to height normalize all acquisitions.
Hudak et al. 2012*	2003, 2007, 2009	No adjustment reported	Height normalization was computed independently for each ALS acquisition. The authors do not report on any assessment of planimetric or vertical differences between acquisitions nor do they report on any adjustments in the pre-processing phase.
Englhart et al. 2013	2007, 2011	No adjustment reported	Assessment of vertical alignment showed differences with 93 control points for both ALS acquisitions, but authors do not report any adjustments. CHM was generated independently for each acquisition.
Bollandsås et al. 2013*	2005, 2008	No adjustment reported	Similar parameters for both ALS acquisitions. Same scan angle and flight altitude. DTMs were generated for each acquisition. The authors do not report on any assessment of planimetric or vertical differences.
Næsset et al. 2013*	1999, 2010	No adjustment reported	Only the 1999 acquisition was vertically aligned using ed to 30 circular control plots on planar road segments. Height normalization was performed independently for each acquisition.
Skowronski et al. 2014	2004, 2006, 2008	No adjustment reported	The authors do not report on any assessment of planimetric or vertical differences between acquisitions nor do they report on any adjustments in the pre-processing phase.
Økseter et al. 2015*	2007, 2010	Use the same DTM to normalize all acquisitions	Used data from 2010 to normalize both acquisitions.
Magnussen et al. 2015*	1999, 2010	2010 point cloud density thinned to match the 1999 density	The authors implemented a thinning of the 2010 ALS to match the density of the 1999 ALS to account for different ALS point densities prior to generating CHM (and deriving height metrics).
McRoberts et al. 2015*	1999, 2010	No adjustment reported	The authors report vertical adjustment for the first ALS acquisition only.
Cao et al. 2016	2007, 2013	Use the same DTM to normalize all acquisitions	Used data from 2013 to normalize both ALS acquisitions. A road transect was used for the calibration.
Zhao et al. 2018	2002, 2006, 2008, 2012	Post hoc adjustment to individual tree heights	Did not assess DTM or co-register point clouds. Developed an empirical correction method at the individual tree level to adjust for height bias (based on different ALS point densities). Different densities were found to have no impact on area-based assessments.
Poudel et al. 2018	2007, 2012	No adjustment reported	The authors do not report on any assessment of planimetric or vertical differences between acquisitions nor do they report on any adjustments in the pre-processing phase. Accounted for different ALS point densities when generating CHM.
Dalponte et al. 2019	2007, 2011	Use the same DTM to normalize all acquisitions	Used DTM from 2007 to normalize both ALS acquisitions.
Esteban et al. 2019*	2010, 2016	No adjustment reported	The authors do not report on any assessment of planimetric or vertical differences between acquisitions, nor do they report on any adjustments in the pre-processing phase. Accounted for different ALS point densities when generating CHM (and deriving metrics).

Can. J. For. Res. **52:** 1334–1352 (2022) | dx.doi.org/10.1139/cjfr-2022-0055

Table 1. Continued

Study	ALS data	Approach	Comments
Mauro et al. 2019	2009, 2015	No adjustment reported	DTMs were created independently. The authors report the accuracy of the DTM but they did not report any adjustments in the pre-processing phase.
Tymińska-Czabańska et al. 2021	2007, 2012, 2018	Use same DTM to normalize all acquisitions	Used DTM from 2012 to normalize all ALS acquisitions.

Note: DTM, digital terrain model; CHM, canopy height model.
*These studies appear to have used the same input ALS data; however, reported pre-processing may have varied.

steep topography, or as a result of an instrument or human error (Stereńczak et al. 2019). Luoma et al. (2017) found that the precision of field-measured tree heights among experienced field crews in boreal forests was approximately 0.5 m (2.9%). Wang et al. (2019) found that field measurements in boreal forests overestimated tree heights, particularly heights of tall trees in a co-dominant crown class (by an average of 0.52 m), as well as heights of smaller trees in intermediate and suppressed crown classes. Field-based measures were found to be more sensitive to stand complexity, crown class, and species than measures derived from ALS. Jurjević et al. (2020) likewise examined the accuracy of field-measured heights in deciduous-dominated forests, finding that field measurements underestimated the heights of co-dominant and intermediate deciduous trees by 1 m. The accuracy of field-measured tree heights has implications for deriving of tree and stand attributes such as volume, biomass, or carbon stocks from ALS data (Hunter et al. 2013; Tompalski et al. 2014). In addition to precise individual tree measures, adequate plot size, plot-positioning accuracy, and representativeness of the complexity of the study area are critical considerations for the collection of accurate ground information and development of area-based forest inventory attributes (White et al. 2013). In the case of multi-temporal ALS data, ground plot measurements errors can be propagated over spatial and temporal scales — in space because of expansion factors used to scale up individual tree measures to plot-, stand-, or landscape-level estimates of forests attributes, and in time due to cumulative errors that may be amplified when changes in forest attributes are quantified (Van Laar and Akça 2007). For these reasons, ALS data has emerged as a more consistent and precise source of information for characterizing forest height growth (Hopkinson et al. 2008).

Given the increasing availability of repeat ALS surveys, we now have new opportunities to use these data to characterize height growth; however, as ALS data acquisitions vary, ensuring that acquisition parameters or data characteristics do not exacerbate uncertainty or error in derived estimates of forest growth requires robust assessment and pre-processing (Coops et al. 2021). As summarized in Table 1, discrepancies between ALS acquisitions — and the subsequent actions taken to account for these differences in studies involving height growth and change — are not commonly assessed or reported in the literature. Moreover, we are not aware of any studies that have quantified the impact of not accounting for these differences in subsequent assessments of height growth. Therefore, our objectives were to (1) assess and quantify the magnitude of the horizontal and vertical differences across four ALS data sets acquired over a 13-year period in a temperate mixedwood forest environment, (2) develop a workflow for harmonizing multi-temporal ALS data sets to account for differences in data acquisition parameters to minimize error in the assessment of change in canopy height, (3) calculate periodic annual increments (PAI) of canopy height and quantify the impact of the harmonization on the derived PAI, and (4) compare and examine inconsistencies between field-measured heights and derived height increments with measures and increments derived from ALS.

2. Materials and methods

2.1. Study area

The Petawawa Research Forest (PRF) is the oldest continuously operated national research forest in Canada (Place 2002). The research forest was established in 1918 in the Great Lakes – St. Lawrence forest region in southern Ontario and occupies approximately 10 000 ha of a diverse temperate mixedwood forest located in a transition zone between boreal forest dominated by coniferous species to the north and deciduous-dominated temperate hardwood forests to the south (Fig. 1). Species diversity and long-term silviculture history characterize the structural complexity of stands in PRF, with a combination of experimental plots, plantations, and application of long-term management plans (White et al. 2019). Common tree species include coniferous species such as jack pine (*Pinus banksiana* Lamb.), white pine (*Pinus strobus* L.), red pine (*Pinus resinosa* Ait.), white spruce (*Picea glauca* (Moench) Voss), and eastern hemlock (*Tsuga canadensis* L.), while deciduous species include trembling aspen (*Populus tremuloides* Michx), sugar (*Acer saccharum* Marsh), and red maple (*Acer rubrum* L.), red oak (*Quercus rubra* L.), and white birch (*Betula papyrifera* Marsh), among others (Wetzel et al. 2011). The PRF has mean annual precipitation of 859 mm, mean annual temperature of 5.6 °C, and ranging in elevation from 140 to 280 m above sea level. Topography is moderately variable and is a product of glaciation and glacial outwashing (White et al. 2021*b*).

2.2. ALS data acquisitions

Four ALS acquisitions were available for the PRF and were acquired in 2005, 2012, 2016, and 2018 during leaf-on periods. Table 2 details the acquisition specifications and

Table 2. Summary of the four ALS data acquisitions.

Data characteristic	ALS_{2005}	ALS_{2012}	ALS_{2016}	ALS_{2018}
Acquisition month	September	August	July	July
Sensor	Leica ALS40	Riegl Q680i	Optech Titan	Leica SPL100
Sensor type	LML	LML	M-ALS	SPL
Horizontal projection	UTM Zone 17 N	UTM Zone 18 N	UTM Zone 18 N	UTM Zone 18 N
Horizontal datum	NAD83 (CSRS)	NAD83 (CSRS)	NAD83 (CSRS)	NAD83 (CSRS)
Vertical datum	NAVD88	CGVD28	CGVD28	CGVD2013
Average point density (points·m^{-2})	0.5	10	5 (second channel only)	32
Average flying altitude (m a.g.l.)	2740	750	1100	3760
Maximum pulse repetition frequency (kHz)	32	150	375	60
Scan angle (°)	±20	±20	±20	±15
Laser wavelength (nm)	1064	1550	1064	532

Note: LML, linear-mode LiDAR; M-ALS, multi-spectral airborne laser scanning; SPL, single photon LiDAR.

confirms that they differed in terms of vertical datum, spatial referencing, and point density. The point density was highest for the ALS_{2018} data with 32 points·m^{-2}, followed by 12 points·m^{-2} for ALS_{2012}, 5 points·m^{-2} for ALS_{2016}, and the lowest for ALS_{2005} with 0.5 points·m^{-2}. The ALS_{2016} data were acquired using the multispectral lidar instrument (Optech Titan) that collects data in three individual channels at the respective wavelengths of 532, 1064, and 1550 nm (see Budei et al. (2018) for details). In this study, only the second channel (1064 nm) was used. The ALS_{2018} data were acquired using a SPL instrument (Leica SPL100).

2.3. Field plot data and processing

In total, 175 circular, fixed-area plots (14.1 m radius, 625 m^2) were established in 2012 and re-measured in 2018 (measurements were performed in leaf-on and leaf-off conditions). These temporary sample plots (TSP) were located to cover the full range of species composition and stand development following a structurally guided sampling approach (White et al. 2013). We aggregated TSP to four main forest types: coniferous dominated, deciduous dominated, mixedwood, and plantations (Table 3). The plot locations were remeasured in 2018 using a TopCon™ GPS unit and post-processed using the Canadian Spatial Reference System Precise Point Positioning Tool (Natural Resources Canada 2020). All stems >9.1 cm in diameter were measured for diameter at breast height over bark. Tree height was measured using a Vertex hypsometer for a subsample of trees (free from any visible top damage), with the four largest trees of the dominant species and the two largest trees of the codominant species measured at each plot. For each tree additional attributes were recorded including species, tree status (live, dead, fallen down, harvested), species, origin (natural, planted, coppice, layering), crown class (co-dominant, dominant, emergent, intermediate, over-topped/suppressed, anomaly), and the decay class for dead trees. Stand-level variables were calculated from tree measurements (Table 3). Top height (H_{TOP}) was calculated as the average height of the six thickest trees per plot, except for managed and natural pine stands (coniferous-lead stands in Table 3), wherein H_{TOP} was calculated as the average height of the two thickest trees per plot. At PRF, a uniform shelterwood silvicultural system is frequently applied to natural and managed pine stands, leaving a few large trees remaining in the stand following harvesting interventions. In these shelterwood stands, H_{TOP} may be biased when heights of these residual tall trees are combined with the heights of the trees in the main canopy, which also results in an overestimation bias in height from the ALS data (White et al. 2021*a*). We found missing height measures for at least one of the six thickest trees in 68% of the plots in 2012 and 56% in 2018. Therefore, we used generalized height–diameter models to complete missing height data in the inventories and maintain a consistent calculation of top height to avoid bias due to a selection effect (García 1998; Magnussen 1999). Generalized height–diameter models based on the formulation of Sharma and Parton (2007) were fit for each species to impute missing tree heights. We used nonlinear mixed-effects models to consider the hierarchical levels of the data (multiple trees in a plot) and relax the assumption of independence (Pinheiro and Bates 2000). We examined graphs of the residuals and fitted values to check for heteroscedasticity and any lack of fit. Among the height–diameter models fitted, jack pine showed the smallest root mean squared error (RMSE) with 1.24 m and white pine showed the highest RMSE value with 1.9 m.

2.4. Time series ALS harmonization

To utilize the multiple ALS acquisitions for forest height growth estimation, we first assessed the planimetric and vertical differences between the different ALS acquisitions. Based on this assessment, we developed a harmonization approach for pre-processing the ALS data to account for these differences prior to generating point cloud metrics and deriving height increments (Fig. 2).

Our harmonization approach involved the following four steps:

1. Horizontal projections and vertical datum transformations: The four independent ALS acquisitions had different spatial referencing and vertical datums (Table 2). Based on an assessment of the quality of PRF terrain models (DTM) in White et al. (2021*b*), the ALS2012 data were selected as

Fig. 1. Location of re-measured temporary sample plots (TSP) in the Petawawa Research Forest (PRF). Figures are produced with ArcGIS Pro 2.7.0; background map credits: Esri, NASA, NRCan, and other contributors. [Colour online]

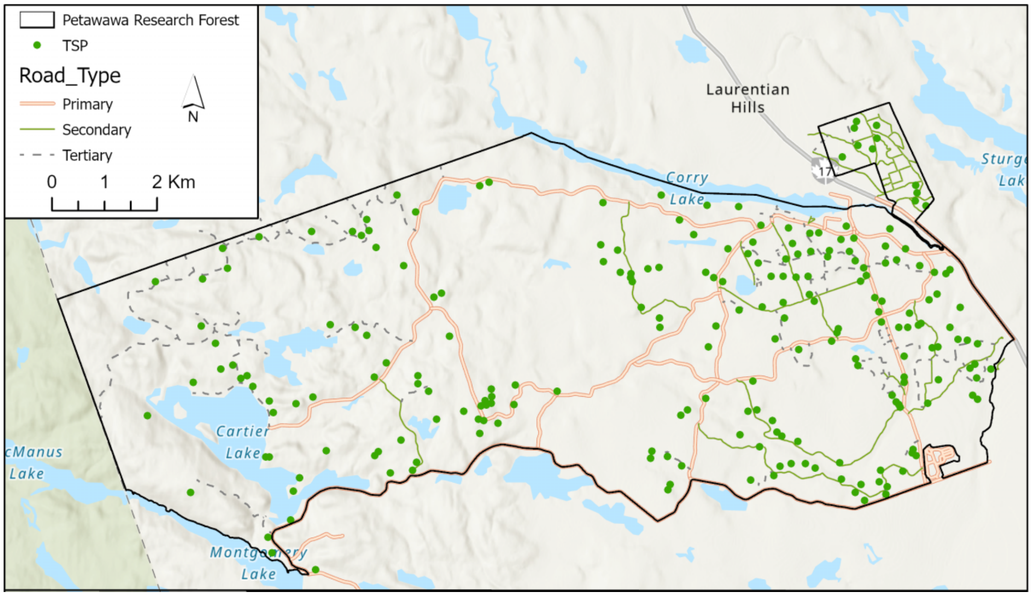

Table 3. Summary of field plot data.

Forest type	No. of plots	Basal area ($m^2 \cdot ha^{-1}$)	Quadratic mean diameter (cm)	Top height (m)	Maximum height (m)	Description
Coniferous-lead	78	28.4 (0.45–78.1)	27.5 (10.2–68.2)	28.7 (8.1–43.0)	30.3 (8.2–43.0)	Natural and managed stands dominated by white pine, red pine, and black spruce often with an understory of poplar and hardwoods.
Deciduous-lead	34	25.8 (0.27–40.9)	23.0 (11.1–36.7)	23.4 (11.9–32.05)	26.0 (11.9–35.2)	Natural deciduous stands with a range of structural conditions dominated by oak, trembling aspen, sugar maple, or beech, and often mixed with other hardwoods and conifers.
Mixedwoods	29	20.7 (2.67–38.1)	18.1 (11.3–23.1)	20.9 (9.6–27.8)	24.5 (12.2–35.4)	Mixed-species plots with a range of species composition proportions of red maple, white spruce, and balsam fir, among others.
Plantations	34	29.1 (10.2–58.2)	21.9 (11.3–49.0)	19.5 (6.5–33.6)	21.8 (6.8–37.2)	Plantations of red pine, jack pine, white pine, and spruce with different initial planting densities and subsequent management activities.

Note: The mean value is followed by the range of values in parentheses.

the reference for harmonization. All ALS data sets were projected to UTM Zone 18 N and then transformed to the same vertical datum as the ALS2012 (CGVD28) using PDAL (version 1.9.1). We then assessed the planimetric and vertical alignment of all four data sets. While we observed no planimetric shifts in permanent features (e.g., buildings, roads), differences in elevation (*z*) of those features were often significant. Data for all ALS acquisitions were tiled using the same tiling scheme (i.e., 1 km × 1 km tiles, no buffers, same naming convention), with processing performed using LAStools software (Isenburg 2021).

2. Vertical alignment: DTMs were generated with a 1 m spatial resolution for all ALS acquisitions using returns classified as ground. To quantify the average elevation difference between resulting DTMs, point samples were located along primary paved roads distributed throughout the PRF (Fig. 1), similar to the approach applied in Hopkinson et al. (2008). Point samples were located every 50 m along the road, which resulted in a total of 4183 points used to calculate the mean difference in elevation between the reference DTM2012 (derived from ALS2012) and each of the three remaining data sets. The three mean difference values for each acquisition relative to DTM2012 were then used to adjust point cloud elevations of ALS2006, ALS2016, and ALS2018, using the translate_z parameter in LAStools las2las function.

Fig. 2. Overall scheme for multi-temporal ALS harmonization compared with non-harmonized data used in this study. (1) Vertical datum transformation. (2) Vertical alignment. (3) Height normalization. (4) Plot/grid metrics calculation. (5) Periodic annual height increments (PAI) were then derived from harmonized and non-harmonized data sets. [Colour online]

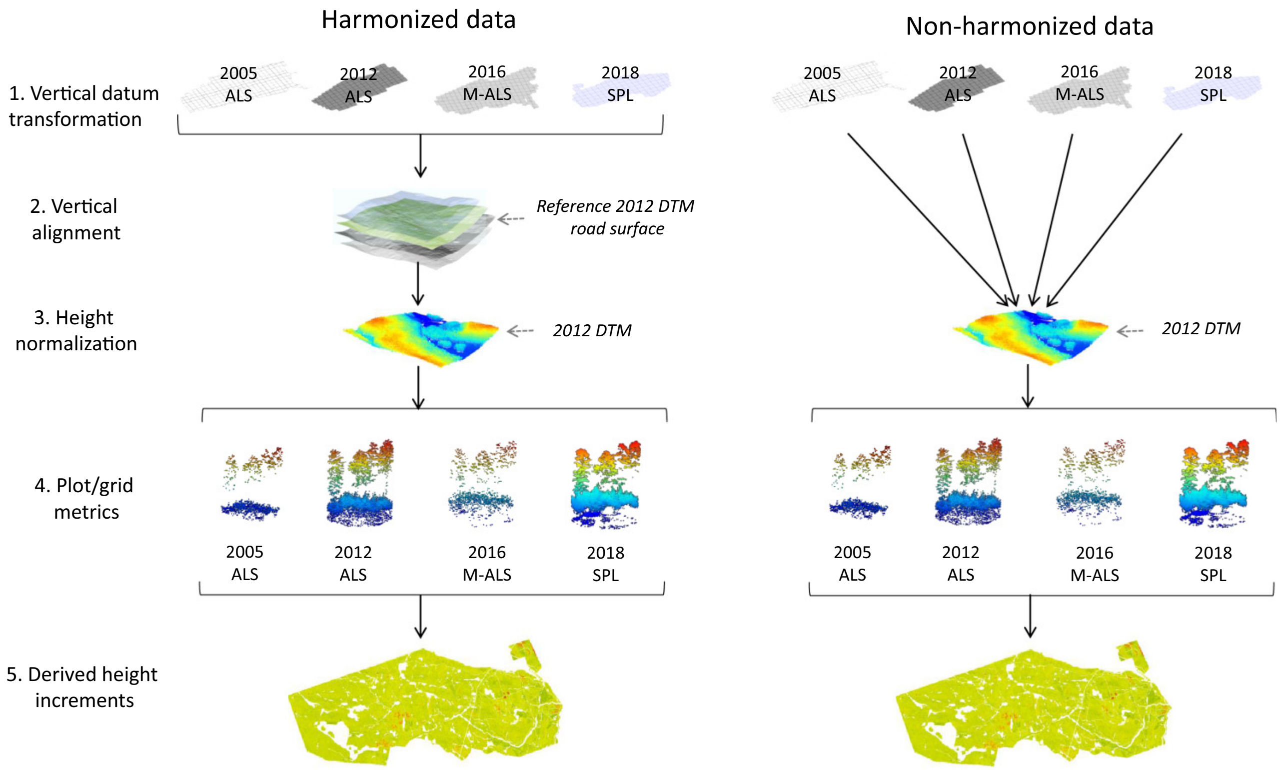

3. Height normalization: We then used DTM2012 as a reference to normalize point cloud heights for all ALS acquisitions to heights above ground level.
4. Generation of point cloud metrics: We used the 99th percentile of the canopy height returns (zq99) to measure height and height growth increment at the plot level. We found the strongest correlation between zq99 and top height compared with other upper percentiles (from the 80th to the 99th). The zq99 metrics for the point cloud corresponding to the fixed-area TSP locations and wall-to-wall with a 25 m grid were generated using only the first returns with the lidR package for R (Roussel et al. 2020).

To assess the impact of our harmonization approach on our assessment of height growth, we also generated a non-harmonized data set (Fig. 2). For the non-harmonized data, we did not transform the vertical datum (step 1) or perform any vertical alignment (step 2). However, all ALS acquisitions were projected to the same horizontal projection system and were height normalized using the ALS_{2012}-based reference DTM. Plot-level metrics were generated and used to interrogate differences between harmonized and non-harmonized ALS data.

We calculated the difference between harmonized and non-harmonized zq99 for each acquisition year and used a Student's t test to evaluate whether the mean differences were significantly different from 0. If the confidence intervals of the difference were within 0, we considered that height metrics were equal between harmonized and non-harmonized data.

2.5. Derivation of PAI from ALS data

Based on the zq99 metric, we calculated height increments for each TSP. The PAI (m·year^{-1}) among different growth periods was calculated as the height difference between any of the ALS data sets, divided by the time interval between acquisitions, assuming constant growth within the period. We compared the PAI values between harmonized and non-harmonized data sets for each period using a pairwise Student's t test. In addition, we used one-way analysis of variances (ANOVAs) with linear mixed-effects models followed by Tukey's post hoc test to determine differences in PAI values among periods for harmonized and non-harmonized data. In our mixed-effect models, the growth period was specified as a fixed effect and the field plot was included as a random effect (Pinheiro and Bates 2000). Field plots that experienced a height reduction exceeding 5 m between 2005 and 2018 ($n = 6$) were considered to have had some form of management or disturbance and were excluded from the PAI computations. Disturbances or management interventions induce a long tail distribution of increment height rate that may mask the differences between harmonized and non-harmonized data.

Table 4. Mean and standard deviation (in brackets) of the difference between harmonized and non-harmonized zq99 for each ALS acquisition.

Data set	df	zq99 (m), mean (standard deviation)	*p* value	CI_{95}
ALS_{2005}	171	0.525 (0.018)	>0.0001	0.522 – 0.527
ALS_{2016}	174	− 0.790 (0)	>0.0001	− 0.790 – −0.790
ALS_{2018}	174	− 0.187 (0.005)	>0.0001	− 0.187 – −0.186

Note: *p*-values ≤ 0.05 indicate that the mean ratio was significantly different from zero. CI95, ±95% confidence intervals.

2.6. Comparison of ALS-derived and field-measured height increments

Height and height increments derived from ALS data were compared with field-based measurements for both 2012 and 2018. H_{TOP} values calculated from field measurements were compared to the zq99 at the plot level. Comparisons were summarized for all the plots pooled together and by forest type. Field and ALS height estimates were compared independently for 2012 and 2018, while height increment was compared for the period 2012–2018, calculated as the difference between H_{TOP} (ΔH_{TOP}) and zq99 values (ΔH_{ALS}). We computed comparisons based on linear relationships between both field and ALS data and quantified the magnitude of inconsistencies between ground and ALS height measurements across different H_{TOP} classes and forest types. The R^2 of the fitted models and the absolute and relative RMSE, considering the ALS measurements as the observed values, were calculated for height and height increments.

A general function of height growth dependent upon plot height was used to illustrate the height growth pattern according to classical growth theory (Pretzsch 2020*a*). We used an established function to depict the growth trajectory of the plots based on expansion and reduction components:

$$\Delta H_M = \beta_0 H \cdot e^{\beta_1 H} + \epsilon \tag{1}$$

where ΔH_M is the height increment modelled and H is the plot height at the beginning of the growing period, β_0 and β_1 are the expansion and reduction parameters of the function, respectively, and ϵ is the residual error term. The behaviour of modelled height growth trajectories was compared using H_{TOP} and H_{TOP} increment (ΔH_{TOP}) for field data, while zq99 and zq99 increment (ΔH_{ALS}) was used for ALS data. Unusual height growth values according to the expected growth trajectory were identified to interrogate both field-measured tree heights and ALS height metrics.

3. Results

3.1. Time series ALS harmonization

For the harmonized ALS data, assessment of the vertical alignment of the ALS-derived DTMs following the vertical datum transformation indicated that DTM_{2005} elevations were on average 0.359 m greater than the DTM_{2012} reference, whereas the DTM_{2018} elevations were 0.084 m greater than the DTM_{2012}. In contrast, the DTM_{2016} elevations were on average 0.79 m less than DTM_{2012}. Vertical adjustments to the point cloud elevations (step 2 in Fig. 2) were, therefore, −0.359, 0.79, and −0.084 m for the ALS_{2005}, ALS_{2016}, and ALS_{2018} data sets, respectively.

Following normalization to heights above ground, plot-level zq99 values between harmonized and non-harmonized ALS data were compared (Table 4). On average, the harmonized zq99 was 0.52 m less than the non-harmonized zq99 for ALS_{2005}, whereas for ALS_{2016} and ALS_{2018} the harmonized zq99 values were 0.79 and 0.19 m greater than the non-harmonized zq99, respectively. The differences between the harmonized and non-harmonized data sets were not constant and showed some variability for the ALS_{2005} (SD = 0.018 m) and ALS_{2018} data (SD = 0.005 m) (Table 4), resulting from the vertical datum transformation. For all acquisitions, the differences between the harmonized and non-harmonized data were significant.

3.2. PAI derived from harmonized and non-harmonized data

The effect of data harmonization on total growth (2005–2018) indicated statistically significant differences between the total growth estimated from the harmonized and non-harmonized ALS data (Table 5). The pairwise comparison showed that on average a height increment from harmonized data (2.63 m) was 0.71 m greater than an average height increment derived from the non-harmonized data (1.92 m) over the entire growing period. The same pattern was observed by forest type, with the greatest difference for coniferous lead (0.714 m) and the smallest difference for plantation (0.703 m) (Table 5).

We also compared the differences in PAI calculated from harmonized and non-harmonized data for different growth periods that could be identified between the four ALS acquisitions (i.e., 2005–2018, 2005–2012, 2005–2016, 2012–2016, 2012–2018, and 2016–2018). We found significant differences in height increments between both data sets for all periods (Fig. 3). For all periods except one, the PAI values were greater for the harmonized data than for the non-harmonized data, with the largest differences for 2012–2016 ($0.198\ m{\cdot}year^{-1}$) and the smallest difference for 2012–2018 ($0.031\ m{\cdot}year^{-1}$) period. For the 2016–2018 period, the PAI was greater for the non-harmonized data ($0.634\ m{\cdot}year^{-1}$) than for the harmonized data ($0.332\ m{\cdot}year^{-1}$). Periods with

Table 5. Total height increment for the period 2005–2018 and standard deviation (in brackets) for harmonized and non-harmonized data sets.

Forest type	Total height increment (2005–2018), mean (standard deviation): Harmonized	Non-harmonized	*p* value
Overall	2.63 (2.41)	1.92 (2.41)	0.007
Coniferous-lead	2.31 (2.06)	1.60 (1.65)	0.003
Deciduous-lead	1.90 (1.65)	1.70 (2.52)	0.016
Mixedwoods	1.70 (2.52)	0.99 (2.53)	>0.0001
Plantation	4.83 (2.38)	4.13 (2.38)	>0.0001

Note: Results are summarized for all forest types (overall) and by forest type. *p*-values $\leq$ 0.05 indicate a significant difference between harmonized and non-harmonized data.

Fig. 3. Comparison between harmonized and non-harmonized data among different growth periods. Asterisks show significant differences (*, $p \leq 0.05$; **, $p \leq 0.01$; ***, $p \leq 0.001$; ns, $p > 0.05$) of the pairwise Student's *t* test within periods.

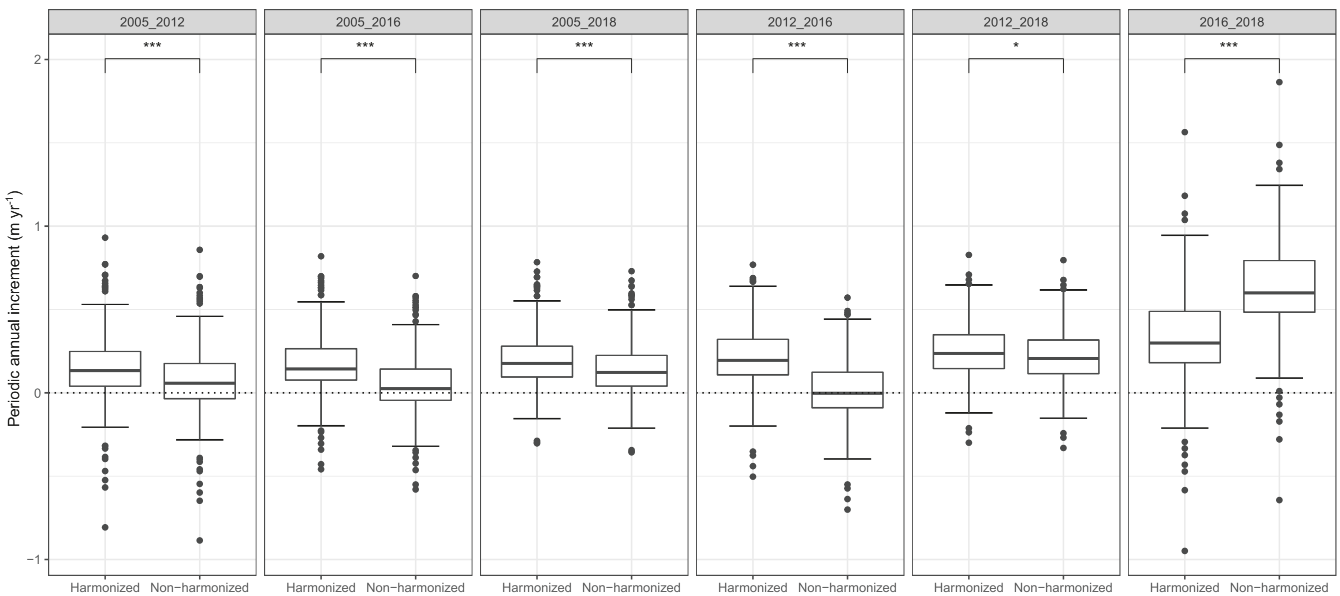

shorter intervals (2016–2018 and 2012–2016) exhibited larger differences between harmonized and non-harmonized data (0.302 and 0.198 m·year^{-1}, respectively), when compared to the increments derived for the longer growth periods (for 2005–2018 and 2005–2016, 0.055 and 0.120 m·year^{-1}, respectively).

We also compared PAI between growth periods within each of the harmonized and non-harmonized data series, respectively (Fig. 4). We observed that PAI values for harmonized data were more consistent among growth periods than for non-harmonized data. PAI calculated from harmonized data were not significantly different among growth periods starting in 2005 or 2012, and for most periods with overlapping years. In contrast, PAI derived from non-harmonized data showed a clear distinction in the calculated PAI among growth periods with a common initial year (i.e., for periods starting in 2005 versus 2012) and with overlapping years. Moreover, PAI in the period 2016–2018 for the harmonized and non-harmonized data was different from PAI for all other growth periods.

3.3. Comparison of ALS- and field-derived height and height increment

We used harmonized data to compare plot height (zq99) and height increment (ΔH_{ALS}) derived from the ALS time series with field plot measurements in 2012 and 2018. For both ALS_{2012} and ALS_{2018}, the zq99 was strongly related to field-measure H_{TOP}, with a mean difference of 0.6 and 0.5 m, respectively, and R^2 of 0.90 and 0.88, respectively (Fig. 5). A similarly strong relationship was observed for the different forest types, with lowest values of R^2 for mixedwoods ($R^2 = 0.7$ and 0.57 in 2012 and 2018, respectively). However, the absolute and relative RMSE indicated greater differences in coniferous-leading and mixedwoods plots compared with deciduous-leading and plantation plots. Despite the strong linear relationship between ground- and ALS-based height estimates, coniferous-leading plots had the highest RMSE values of 2.92 and 3.14 m and a relative RMSE greater than 10% in 2012 and 2018, respectively. Deciduous-leading plots had an RMSE <1.68 m, whereas plantation plots had an RMSE < 1.75 m for both 2012 and 2018.

Can. J. For. Res. **52:** 1334–1352 (2022) | dx.doi.org/10.1139/cjfr-2022-0055

Fig. 4. Comparison of PAI values across growth periods for harmonized and non-harmonized data sets. Different letters denote significant differences in PAI among all periods.

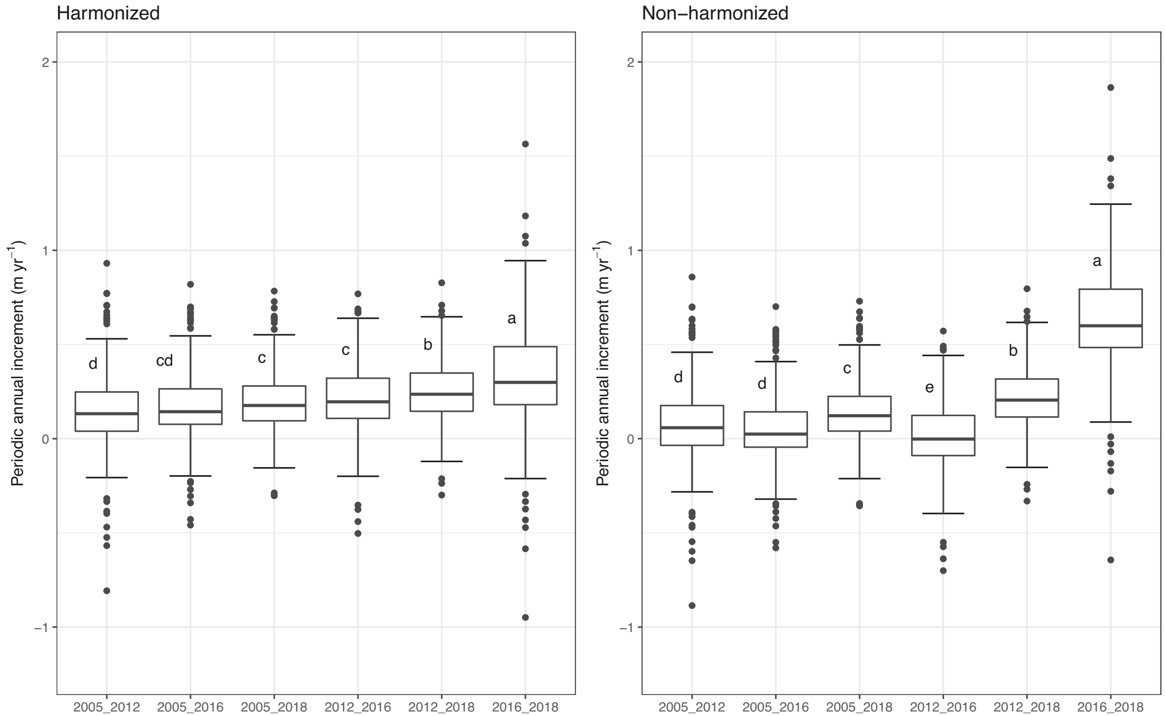

Differences between zq99 and H_{TOP} were not consistent with the H_{TOP} class (Fig. 6*a*). Differences ranged between −13 and 8 m in 2012, and between −11 m and 8.5 m in 2018, with differences increasing with increasing H_{TOP}. Generally, zq99 was lower than H_{TOP}, and this tendency for ALS to underestimate canopy height is well documented in the literature (e.g., Andersen et al. 2006).

The comparison of the ALS- (ΔH_{ALS}) and field-derived height increment (ΔH_{TOP}) between 2012 and 2018 (Fig. 7) showed that the relationship between the two variables was markedly lower (R^2 = 0.12) compared to the strong relationships we observed between zq99 and H_{TOP}. Among forest types, coniferous-lead plots had the weakest relationship between height increments with RMSE of 3.15 m and R^2 = 0.053. Stronger relationships were found for plots located in deciduous-leading and mixedwoods stands (R^2 = 0.38 and 0.33 and RSME = 1.01 and 1.81 m, respectively).

When we modelled the height growth function, we observed two diverging trends for the field and ALS-derived increments (Fig. 8). For the field measurements, we observed that height growth increased with increasing H_{TOP}, whereas for the ALS, height growth decreased with increasing H_{TOP}. We would expect to see decreasing growth increments with increasing H_{TOP} (Weiskittel et al. 2011; Pretzsch 2020*a*); however, for the field data, there were unusually large growth values for plots with H_{TOP} >25 m and extremely large height growth increments (i.e., >5 m) for plots with H_{TOP} >40 m (Fig. 6*b*). A similar trend was observed for the coniferous-leading plots, whereas the deciduous-leading plots showed a more constant growth rate relative to increasing H_{TOP}. Trends for mixedwoods and plantations were more consistent between the field- and ALS-derived increments (Fig. 8). We noted that most of inconsistent height growth values from the field plot data were concentrated in coniferous-leading plots, specifically in unmanaged pine stands.

We examined the TSPs with the largest differences between H_{TOP} and zq99 by overlaying the point cloud profiles from the 2012 and 2018 ALS acquisitions (Fig. 9). This comparison showed substantial differences in field measurements of tree height compared to the ALS zq99. The documented examples illustrated that relatively large measurement differences in one or both years resulted in either an overestimation of height growth or negative increment computations when compared with the height increments derived from the ALS data. For example, in unmanaged pine stands dominated by white pine, the field-derived height increment for TSP165 is 6.9 m, compared to 0.78 m from the ALS data. Likewise, the field-derived increment for TSP095 is 11.7 m, compared to 1.63 m from the ALS data. In the case of TSP203, the measurement errors of tree heights in the 2012 field data reflect a marked decrease in height (−3.9 m) when compared to the actual height growth (1.64 m) calculated based on ALS data.

4. Discussion

Herein we demonstrate the impact of ALS pre-processing and harmonization on derived height growth increment. Studies that have used bi-temporal or multi-temporal ALS data for height growth assessments do not commonly consider or report details concerning methods for data harmonization (Table 1). We found that even after careful

Fig. 5. Relationship between H_{TOP} calculated from field plot measurements and zq99 percentile metric in 2012 and 2018, for the forest overall and by forest type. [Colour online]

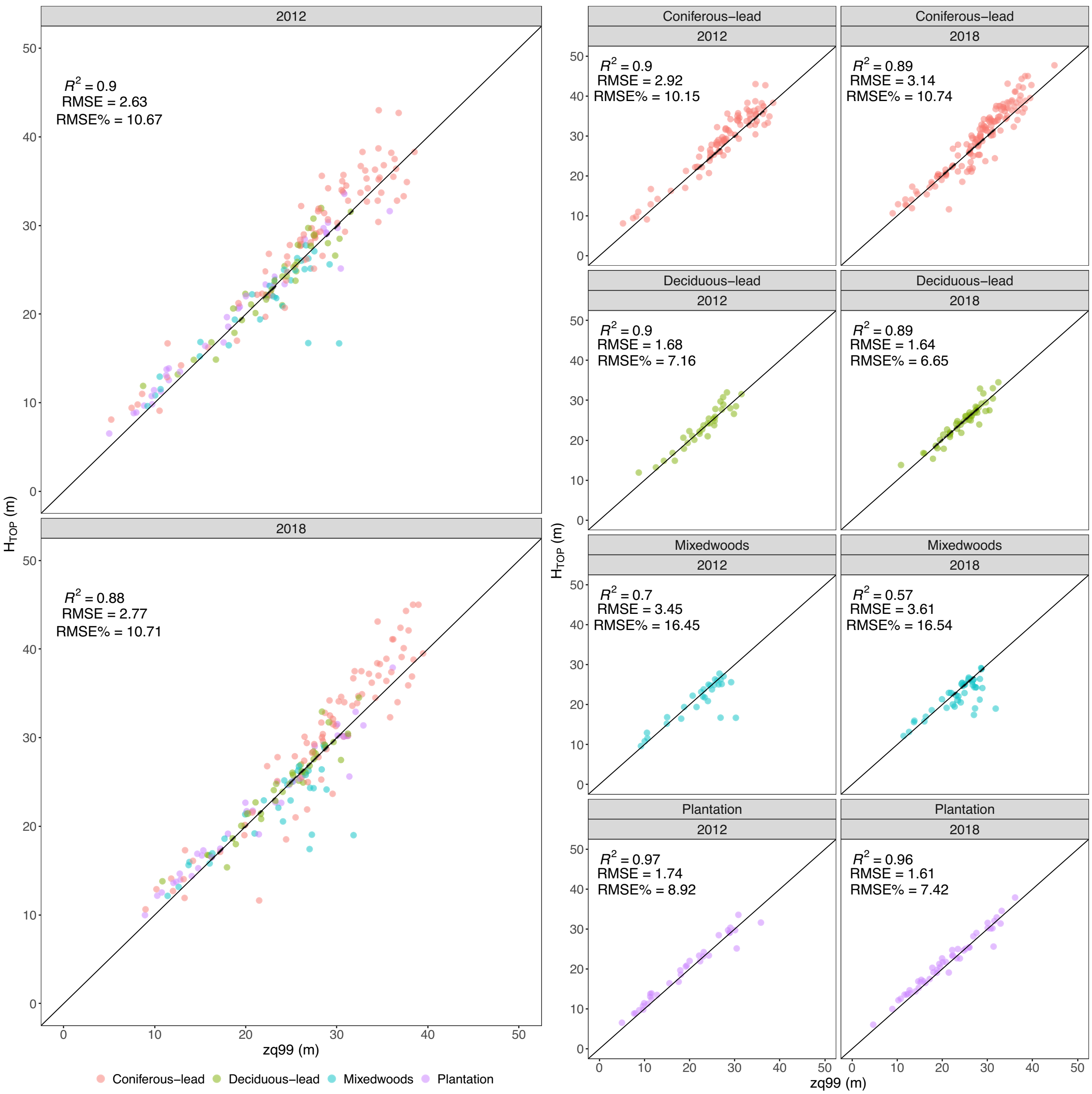

planimetric assessment, projection, and vertical datum transformation, there remained vertical offsets in ground elevations in our various ALS acquisitions for invariant features (paved roads) relative to our selected reference year (2012) and thus we applied a vertical adjustment to each ALS acquisition representing the average difference between that acquisition and the reference DTM. An assumption is often made that terrain surfaces are largely invariant (Yu et al. 2004); however, other factors, including the vertical accuracy of the acquisition, can result in systematic shifts between ALS acquisitions that need to be accounted for prior to growth assessment (Hopkinson et al. 2008).

4.1. Vertical alignment assessment of multi-temporal ALS

The DTM_{2016} had the greatest difference with the reference DTM_{2012} (0.79 m), followed by DTM_{2005} (0.359 m) and DTM_{2018} (0.084 m). Different sensors and acquisition configurations can influence the vertical alignment of ALS (Næsset 2009; Lee and Wang 2018). Each of the data sets used in our assessment was acquired with different instruments and acquisition parameters (Table 2). The ALS acquisitions used in this study had marked differences in average point density, with the last survey in 2018 being 6, 3, and 64 times greater in density than 2016, 2012 and 2005 surveys,

Fig. 6. (*a*) Discrepancies between H_{TOP} calculated from ground measurements and zq99 derived from ALS metrics by 5 m H_{TOP} class in 2012 and 2018. (*b*) Height increment (2012–2018) derived from field and ALS data by 5 m H_{TOP} height class.

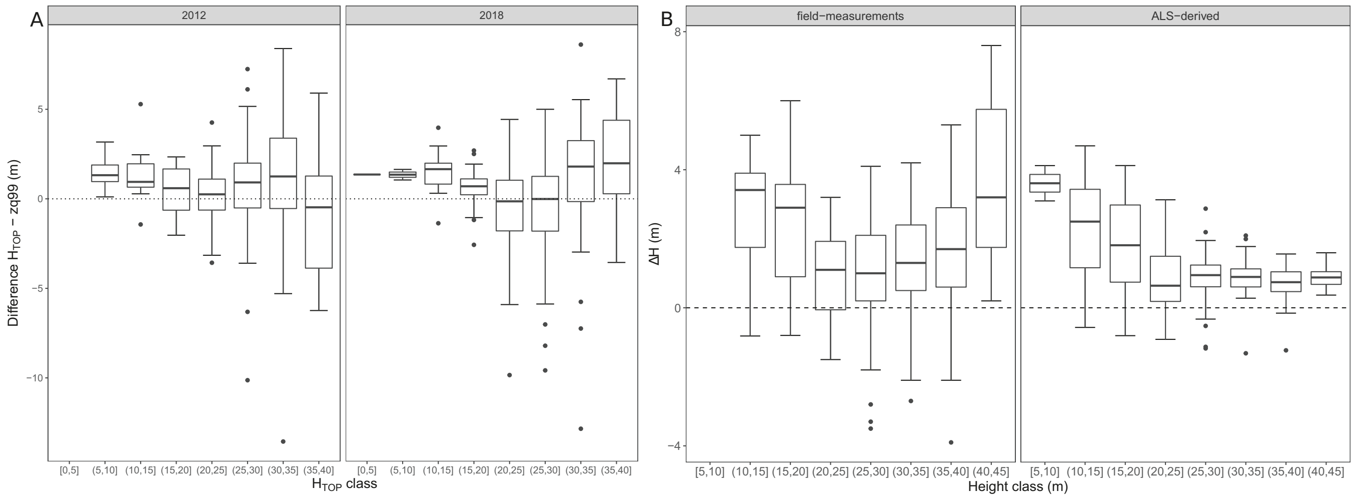

Fig. 7. Comparison of ALS (ΔH_{ALS}) and field-derived (ΔH_{TOP}) height increments, overall and by forest type. [Colour online]

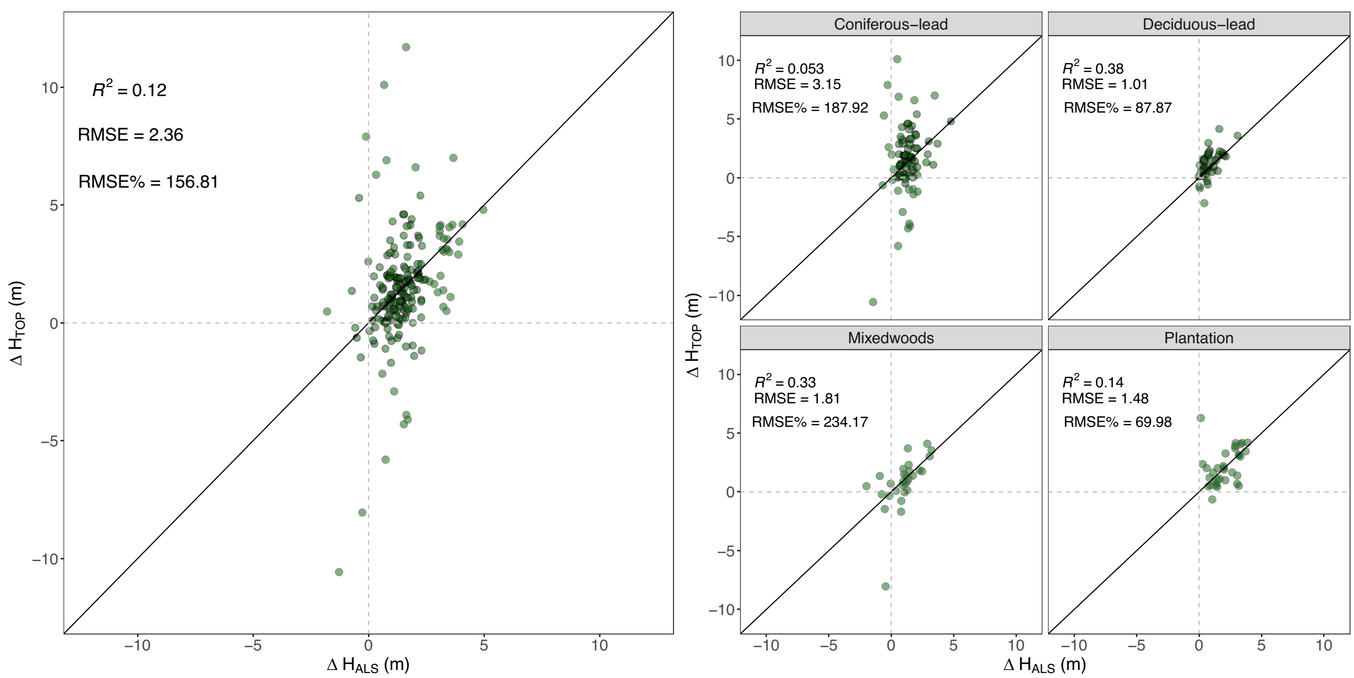

respectively. Although, all ALS acquisitions were acquired in leaf-on conditions, the flight altitude was specific to the sensor technology used for each acquisition. The variability observed between harmonized and non-harmonized data for ALS_{2005} and ALS_{2018} resulted from the model applied for the vertical datum transformation. The differences in vertical datums were not constant across the study area but vary west to east as a function of the transformation models applied. For example, nationally, the differences between CGVD28 and CGVD2013 range from −65 to 55 cm west to east (Natural Resources Canada 2006, 2020). Both the ALS_{2005} and ALS_{2018} point clouds were subject to vertical datum transformation (from NAVD88 to CGVD28 and from CGVD2013 to CGVD28), and the differences between vertical datums had a standard deviation of 0.018 and 0.005 m, respectively. No vertical datum adjustment was applied to the ALS_{2016} data, resulting in a constant difference value for these data.

The magnitude of the correction required for alignment to the DTM_{2012} varied among the different ALS acquisitions; however, it was of similar magnitude to that of other studies undertaken both at the same site and worldwide. Across a subset of the PRF study area, White et al. (2021*b*) observed that the ALS_{2018} SPL data overestimated elevation relative to the ALS_{2012} linear-mode LiDAR (LML) by 0.074 m, in agreement with the mean difference between the ALS_{2012}

Fig. 8. Height increment (ΔH) plotted over height (H) at the beginning of the growing period (2012–2018). Overall and by forest types, height growth trajectories of H_{TOP} increments (ΔH_{TOP}) — H_{TOP} from ground measurements and ALS-derived height increments (ΔH_{ALS}) — height at the plot level (zq99). The respective general height growth pattern modelled by the function in eq. 1 (red line). [Colour online]

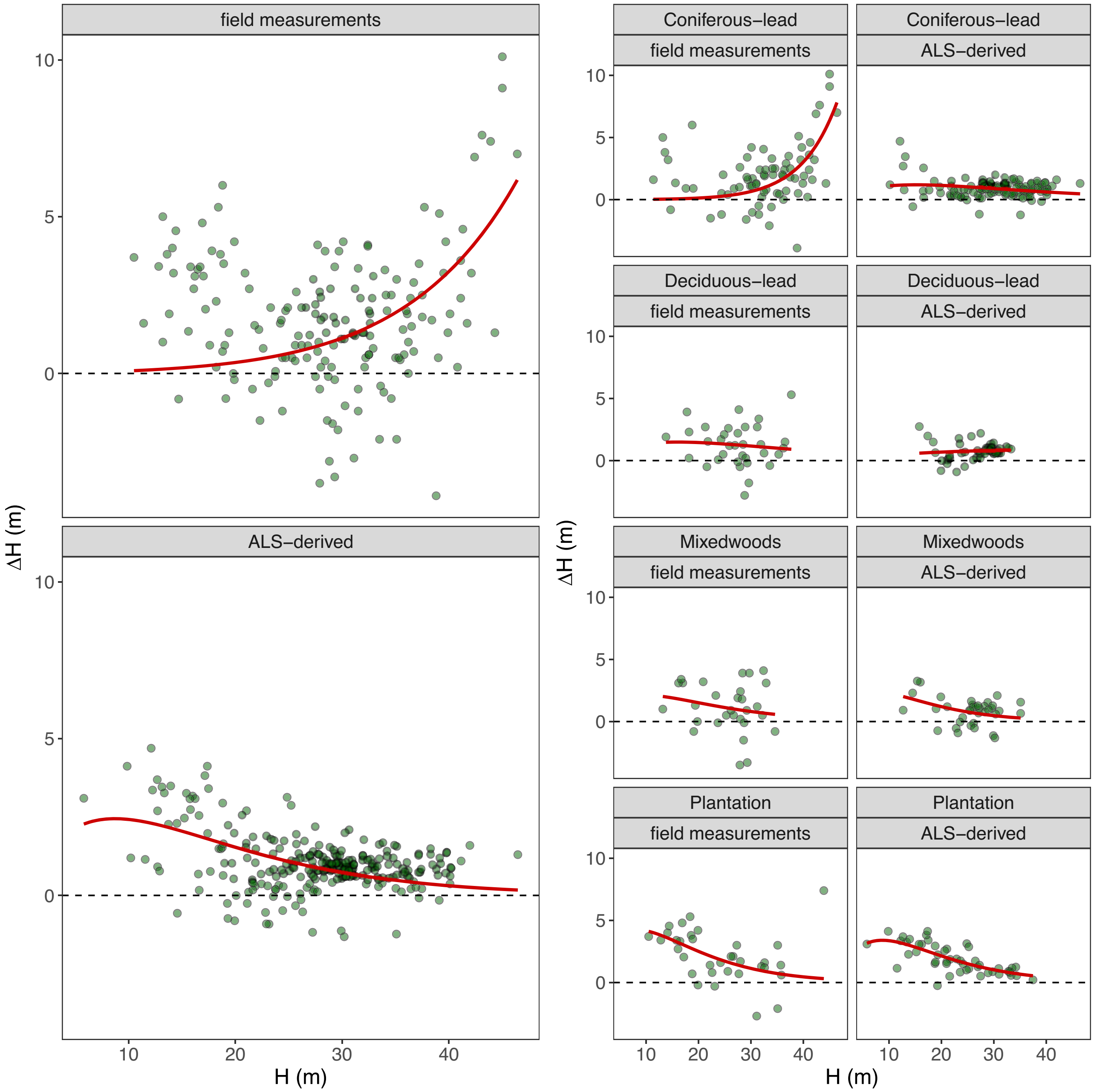

and ALS_{2018} data sets reported in this study (0.084 m). The authors also noted increasing differences between ALS_{2012} LML and ALS_{2018} SPL DTMs with increasing slope. Previously, standardization methods applied in other studies reported both systematic and random errors when comparing DTMs derived from bi-temporal ALS acquisitions (St-Onge and Vepakomma 2004; Næsset and Gobakken 2005; Cao et al. 2016); however, the impact of this vertical misalignment on height growth measurements has not been commonly explored. Yu et al. (2004) used the same sensor and acquisition parameters (Toposys-1 laser scanner from an altitude of 800 m a.g.l. with a pulse repetition of 83 kHz and pulse density of 4.5 points·m^{-2}) for ALS acquisitions in 1998 and 2000. The authors reported up to 0.41 m difference in mean height growth at plot level after the vertical alignment. St-Onge and Vepakomma (2004) evaluated the tree height growth in hardwood and softwood in the mixed boreal forest. They found that the elevation of the 1998 (ALTM1020, pulse repetition frequency 4 kHz, flight altitude 700 m a.g.l., point density 0.03 points·m^{-2}) ground returns was on average 0.22 m higher than the corresponding 2003 returns (ALTM2050, pulse repetition density 50 kHz, flight altitude

Fig. 9. Examples of TSPs with the largest discrepancies between field-measured tree heights and ALS-measured heights. Points cloud from 2012 (purple) and 2018 (green) ALS acquisitions are overlaid and viewed in profile from ground level. Horizontal dashed lines represent the plot top height (H_{TOP}), whereas the solid lines are the ALS-derived zq99 percentile metric (zq99) in 2012 and 2018. [Colour online]

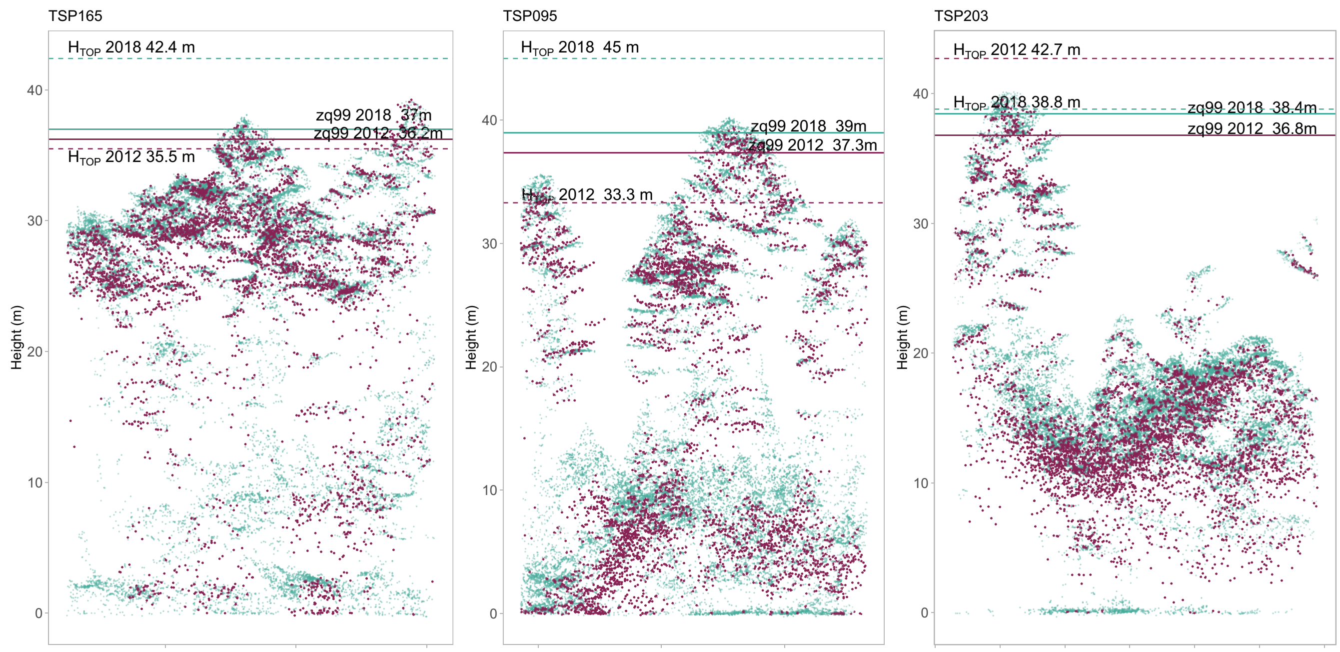

1000 m a.g.l., point density 0.19 points·m^{-2}). Under boreal forest conditions, Næsset and Gobakken (2005) computed a mean difference of 0.137 m comparing the terrain surface model generated for 1999 and 2001 using the same laser scanner (Optech ALTM 1210) and similar acquisition specifications (700–850 m a.g.l., pulse repetition frequency 10 kHz, and 1.18–0.87 points·m^{-2}). In a more recent study, Cao et al. (2016) used two ALS data sets and a single DTM for height normalization, after calibrating the DTMs by the mean height difference (0.103 m) between 2007 (Optech ALTM-3100, pulse repetition frequency 50 kHz, flight altitude 800 m a.g.l., point density 1.93 points·m^{-2}) and 2013 ALS surveys (Riegl LMS-Q680i, pulse repetition frequency 360 khz, flight altitude 900 m a.g.l, point density 8.37 points·m^{-2}). Yu et al. (2004) noted that differences in the DTM could have a significant impact on ALS-derived estimates of height growth and compensated for the difference by using a common reference DTM for normalization to heights above ground. In their study, however, Yu et al. (2004) assessed height growth over a 2-year period, and the authors posited that in boreal forests the average amount of growth over a 5-year period would "make errors arising from the DTM insignificant" and therefore DTM compensation would typically not be required in the growth estimation.

There are conflicting results reported in the scientific literature regarding the effect of scan angle on ALS-derived metrics and models. Using an experimental approach, van Lier et al. (2022) showed that most ALS metrics, including height percentile metrics, were not significantly affected by scan angles less than 20°. We consider that the overlap between adjacent flight lines (~50%) and scan angles (<20°) of the ALS acquisitions used for our study minimizes the influence of scan angle. Likewise, for an area-based approach (i.e., grid cell), as we have implemented herein, differences in point density among acquisitions (Table 2) likely have very little influence on derived ALS metrics because the spatial distribution of the point cloud is similar even if the point density varies markedly (Treitz et al. 2012; Zhao et al. 2018). Furthermore, increasing point density does not increase area-based estimates accuracy (Hudak et al. 2012; Jakubowski et al. 2013) and plot size has been shown to have a greater effect than density when estimating forest structural attributes (Ruiz et al. 2014).

4.2. Impact of harmonization on derived PAI

Over the entire growth period (2005–2018) differences in growth increments between the harmonized and non-harmonized data sets were statically significant, with harmonized data sets resulting in height growth increments that were on average 37% greater than those derived from non-harmonized data. We likewise found significant differences between PAI derived from harmonized and non-harmonized data for all other periods considered. Only for the period 2016–2018 was PAI greater for the non-harmonized than harmonized data; however, this difference likely results from the larger misalignment of the DTM_{2016} compared with the DTM_{2012} (−0.79 m), which exceeds the total height growth for the period (0.66 m). Consequently, the lower height of point clouds in 2016 resulted in an overestimation of the height increment for the non-harmonized data.

Interestingly, we also noted that for shorter growing intervals there were larger differences in PAI between harmonized and non-harmonized data. For instance, 0.293 m·year^{-1} for the 2-year period 2016–2018 compared to 0.05 m·year^{-1} for the full 13-year period (2005–2018). Yu et al. (2004) analysed tree height growth in the boreal forest for a 2-year interval between ALS surveys and reported that in certain cases, canopy height changes attributed to the use of different terrain models were larger than the changes attributed to canopy height growth. Similar results were shown by Véga and St-Onge (2008), whereby longer time intervals between data acquisitions increased the accuracy of height growth despite errors in canopy height estimates at individual points in time. Although we observed differences in PAI between harmonized and non-harmonized data for all periods, our results support the idea that the shorter the time interval is for assessing growth, the more important is evaluating and compensating for vertical alignment in the ALS data. Moreover, considering that height at both the tree and stand level is a key determinant for estimating volume and biomass and is a useful indicator of forest site quality (Russell et al. 2014), bias in tree height estimates can impact individual-tree volume estimates more significantly than errors in species classification (Tompalski et al. 2014).

Harmonization generated a more consistent PAI series among different periods reducing the uncertainties related to ALS-based systems. Compared to the entire 13-year growing period analysed (2005–2018), growth periods greater than 4 years showed similar PAI values. However, the amount of time necessary for sufficient growth to overcome noise and other uncertainties within ALS systems might depend on growing conditions, development stage, stand structure, and species composition. In stands with a slow growth rate or high level of mortality, height growth can be difficult to quantify correctly if increments are small compared to instrument errors or modelling uncertainty (Tompalski et al. 2019). Moreover, the variability observed in PAI values among periods reflects other factors affecting growth, for instance, climate fluctuations among growth periods, forest management interventions, or intrinsic forest growth dynamics (Bowman et al. 2013; Pretzsch 2020*a*).

4.3. Comparison with height increments from field measurements

Although we found a strong agreement between ALS-derived height and H_{TOP} from field measurements, ALS and field-derived height increments were only weakly correlated. Height, volume, or biomass increments estimated by direct or indirect methods are regularly less accurate than measurements or estimates for a given time (Cao et al. 2016; Tompalski et al. 2019), and correlations between ALS and field measurements might significantly vary with changing stand conditions (Wang et al. 2019). By exploring the more extreme discrepancies between ALS-derived and field measurements, we found both systematic and random differences in the tree height measurements from the field plots (Fig. 9). Systematic differences were observed especially in natural pine stands with an H_{TOP} greater than 25 m (Figs 5 and 6*a*). In the PRF, natural pine stands are characterized by single-layer unmanaged stands with veteran trees in the overstory, with a mix of white and red pine and with an understory of other tree species including poplar, spruce, and hardwoods (White et al. 2021*a*). Under these stand conditions, accurate tree height measurements are challenging to achieve especially for dominant trees due to restricted visibility and hence exceeding the expected mean error of 1.5 m for height measurements reported by Luoma et al. (2017).

Although ALS technology is notable for generating more accurate measurements of tree height compared to field measurements (Ganz et al. 2019; Wang et al. 2019), mapping basic forest structural attributes require the establishment of statistical relationships between field plot information and point cloud metrics (White et al. 2017). Uncertainties associated with field data, such as measurement biases, and sampling errors, will be propagated and accumulate through the height growth calculations, constraining the accuracy of models to describe forest attributes (Zolkos et al. 2013; Fassnacht et al. 2014). In our results, the relative differences between ALS- and field-derived tree height measurements in 2012 and 2018 were smaller than the height increments discrepancies. Moreover, we noted that errors propagated to height increment calculation exceed the actual growth rate, which influenced strongly the discrepancies with ALS-derived PAI. This might have important implications for the performance of direct or indirect methods used for estimating stand growth, especially for slow-growing stands or short time intervals between data acquisitions (Tompalski et al. 2019). Our results indicated that special attention is required prior to using ground plot measurements for growth assessment, and assessing the agreement or bias between both ALS-derived and ground-derived metrics should be considered in the analysis of multitemporal ALS data.

4.4. Considerations in using time series ALS for height growth assessments

The results of our study demonstrate the feasibility of height growth quantification at the plot level in temperate mixedwoods forests based on repeated ALS acquisitions. As shown in Fig. 8, the growth trajectory of the height increment–height function followed the expected behaviour according to classical theory that growth depends on the current state and resource supply (Zeide 1993; Pretzsch 2020*a*). However, the evident variation of the growth trajectory among forest types showed that structure, species composition, and management legacy effects strongly determine the growth rate especially in more complex stands (Pretzsch 2020*b*, 2022). For instance, for uneven-aged or irregular stands, height growth trajectories are expected to follow a different growth pattern than even-aged stands due to different size-diameter and size-height distributions as a result of suppression growth periods that reduced height increment due to overstory competition (Weiskittel et al. 2011).

Implementing the area-based approach (ABA) could lessen the harmonization effect in the derived forest inventory attributes, e.g., top height, because the offset during the vertical alignment between ALS acquisitions represents a constant shift in the means and percentiles of point clouds. Hence, area-based models derived from harmonized and non-harmonized data should not be substantially different. However, in the case of multitemporal ALS acquisitions, the implementation of ABA requires additional considerations. First, the lack of repeated ground inventories for all four ALS acquisitions constrains the straightforward implementation of ABA. Alternatively, models that integrate temporally disparate inventory data with multitemporal ALS data require an analytical framework capable of acknowledging the temporal disjoint explicitly and appropriately propagating the resulting uncertainty (Babcock et al. 2016; Fekety et al. 2015). In addition, the uncertainties associated with the field measurements, the heterogeneity of structures, composition, management, and development stage among stands in our study require special attention to define and test the most appropriate approach to capture the growth variability in the estimations.

From a forest management perspective, multi-temporal ALS data provide unprecedented accurate information at a fine spatial scale on the current state and changes of forest attributes over large areas and time (White et al. 2016). Quantifying and modelling change at high spatial resolutions could be a powerful tool for improving predictions of G&Y models (Penner and Pitt 2019). G&Y models need the capability to ingest and process increasingly available repeated ALS data, which provide information on every tree in a stand, and are not restricted to the range of conditions of the field plot network. Height changes derived from multi-temporal ALS data may be modelled at the plot- or grid-cell level as a function of the initial stand attributes and then projected to height growth and related attributes such as volume and biomass for different forest management scenarios over time. Height growth trajectories extracted from repeated ALS provide the opportunity to develop site productivity estimates (Socha et al. 2017; Guerra-Hernández et al. 2021), especially for more structurally complex forests, often lacking in representation in forest inventories and G&Y models. Moreover, multi-temporal ALS data can provide spatially detailed information on forest demographics, as mortality and recruitment are also important components of assessing forest growth.

There are different ways in which ALS measures of forest structure or ALS-based estimates of forest attributes can be integrated into existing G&Y models, depending on the type of model, input data requirements, and necessary attributes (Tompalski et al. 2021). Alternatively, the development of growth models driven entirely with point-cloud data might offer the possibility to project cell-level attributes to broader range of site conditions and integrate other data sources, for example, digital aerial photogrammetry (Tompalski et al. 2018). Besides the direct applications in a forestry context, including forest operations, inventory, planning, and management, this work contributes novel methodological considerations in the analysis of multi-temporal ALS data to quantify and measure a broad suite of more complex ecosystem characteristics under the paradigm of adaptive forest management (Goodbody et al. 2021).

5. Conclusion

Our results demonstrate that systematic differences in vertical alignment among multi-temporal ALS data sets may result in errors in derived height growth increments and demonstrate that careful assessment and harmonization of multi-temporal ALS should be applied to obtain an accurate assessment of height growth. Both vertical accuracy and consistency between height measurements collected across multi-temporal ALS acquisitions are key aspects to successfully detecting forest height growth. Our results indicated that small but systematic errors in the vertical alignment of repeated ALS acquisitions can result in a biased quantification of PAI. This is especially important when combining data with short-time intervals between acquisitions. As ALS data becomes increasingly common and mature as a data collection option, understanding how best to extract robust information to quantify and relay change over time is required. Accounting for the characteristics of a given ALS data set that are not related to trees or tree growth, such as demonstrated in this research, will enable the generation of accurate products to monitor and forecast forest growth.

Acknowledgements

We thank Hao Chen for his assistance with lidar processing and vertical datum transformation, and Adam Dick for sharing his insights on forest growth information needs. Murray Woods and Dr. Margaret Penner are thanked for compiling and sharing the field data for 2012 and 2018.

Article information

History dates

Received: 25 February 2022
Accepted: 12 July 2022
Version of record online: 6 September 2022

Copyright

Data availability

ALS data and field measurements used in our analysis are openly available on the PRF remote sensing supersite: https://opendata.nfis.org/mapserver/PRF.html.

Author information

Author ORCIDs

José Riofrío https://orcid.org/0000-0003-2278-2851
Michael A. Wulder https://orcid.org/0000-0002-6942-1896

Author notes

This Article is part of a collection entitled Linking Growth Models and Remote Sensing.

Author contributions

José Riofrío: Conceptualization, Data curation, Formal analysis, Investigation, Methodology, Writing — original draft, Writing — review & editing

Joanne White: Conceptualization, Formal analysis, Funding acquisition, Methodology, Resources, Supervision, Writing — review & editing

Piotr Tompalski: Conceptualization, Formal analysis, Methodology, Writing — review & editing

Nicholas Coops: Conceptualization, Funding acquisition, Project administration, Resources, Supervision, Writing — review & editing

Michael Wulder: Conceptualization, Funding acquisition, Project administration, Resources, Writing — review & editing

Competing interests

The authors declare there are no competing interests.

Funding information

This work was supported in part by funds from the Canadian Wood Fibre Centre of the Canadian Forest Service. Field data were collected through funds provided by the Canadian Wood Fibre Centre of the Canadian Forest Service and by the Ontario Forestry Future's Trust.

References

Andersen, H.E., Reutebuch, S.E., and McGaughey, R.J. 2006. A rigorous assessment of tree height measurements obtained using airborne lidar and conventional field methods. Can. J. Remote Sens. **32**(5): 355–366. doi:10.5589/m06-030.

Babcock, C.,Finley, A.O., Cook, B.D., Weiskittel, A., and Woodall, C.W. 2016. Coupling long-term inven- tory and LiDAR data. Remote Sens. Environ. **182**: 1–12. doi:10.1016/j.rse.2016.04.014

Bollandsås, O.M., Gregoire, T.G., Næsset, E., and Øyen, B.H. 2013. Detection of biomass change in a Norwegian mountain forest area using small footprint airborne laser scanner data. Stat. Methods Appl. **22**(1): 113–129. doi:10.1007/s10260-012-0220-5.

Bowman, D.M.J.S., Brienen, R.J.W., Gloor, E., Phillips, O.L., and Prior, L.D. 2013. Detecting trends in tree growth: not so simple. Trends Plant Sci. **18**(1): 11–17. doi:10.1016/j.tplants.2012.08.005.

Budei, B.C., St-Onge, B., Hopkinson, C., and Audet, F.A. 2018. Identifying the genus or species of individual trees using a three-wavelength airborne lidar system. Remote Sens. Environ. **204**: 632–647. Elsevier Inc. doi:10.1016/J.RSE.2017.09.037.

Cao, L., Coops, N.C., Innes, J.L., Sheppard, S.R.J., Fu, L., Ruan, H., and She, G. 2016. Estimation of forest biomass dynamics in subtropical forests using multi-temporal airborne LiDAR data. Remote Sens. Environ. **178**: 158–171. doi:10.1016/j.rse.2016.03.012.

Coops, N.C., Tompalski, P., Goodbody, T.R.H., Queinnec, M., Luther, J.E. Bolton, D.K., et al. 2021. Modelling lidar-derived estimates of forest attributes over space and time: a review of approaches and future trends. Remote Sens. Environ. **260**: 112477. doi:10.1016/j.rse.2021.112477.

Dalponte, M., Jucker, T., Liu, S., Frizzera, L., and Gianelle, D. 2019. Characterizing forest carbon dynamics using multi-temporal lidar data. Remote Sens. Environ. **224**: 412–420. Elsevier. doi:10.1016/j.rse.2019.02.018.

Englhart, S., Jubanski, J., and Siegert, F. 2013. Quantifying dynamics in tropical peat swamp forest biomass with multi-temporal LiDAR datasets. Remote Sens. **5**(5): 2368–2388. doi:10.3390/rs5052368.

Esteban, J., McRoberts, R.E., Fernández-Landa, A., Tomé, J.L., and Næsset, E. 2019. Estimating forest volume and biomass and their changes using random forests and remotely sensed data. Remote Sens. **11**(16): 1944. doi:10.3390/rs11161944.

Fassnacht, F.E., Hartig, F., Latifi, H., Berger, C., Hernández, J., Corvalán, P., and Koch, B. 2014. Importance of sample size, data type and prediction method for remote sensing-based estimations of aboveground forest biomass. Remote Sens. Environ. **154**(1): 102–114. doi:10.1016/j.rse.2014.07.028.

Fekety, P.A., Falkowski, M.J., and Hudak, A.T. 2015. Temporal transferability of lidar-based imputation of forest inventory attributes. Can. J. For. Res. **45**(4): 422–435. doi:10.1139/cjfr-2014-0405.

Ganz, S., Käber, Y., and Adler, P. 2019. Measuring tree height with remote sensing—a comparison of photogrammetric and LiDAR data with different field measurements. Forests **10**(8): 694. doi:10.3390/f10080694.

Garcia, M., Saatchi, S., Ferraz, A., Silva, C.A., Ustin, S., Koltunov, A., and Balzter, H. 2017. Impact of data model and point density on aboveground forest biomass estimation from airborne LiDAR. Carbon Balance Manag. **12**(1): 1–18. doi:10.1186/s13021-017-0073-1. PMID: 28413845.

García, O. 1998. Estimating top height with variable plot sizes. Can. J. For. Res. **28**(10): 1509–1517. doi:10.1139/x98-128.

Goodbody, T.R.H., Coops, N.C., Luther, J.E., Tompalski, P., Mulverhill, C. Frizzle, C., et al. 2021. Airborne laser scanning for quantifying criteria and indicators of sustainable forest management in Canada. Can. J. For. Res. **51**: 1–14. doi:10.1139/cjfr-2020-0424.

Guerra-Hernández, J., Arellano-Pérez, S., González-Ferreiro, E., Pascual, A., Sandoval Altelarrea, V., Ruiz-González, A., and Álvarez-González, J. G. 2021. Developing a site index model for P. Pinaster stands in NW Spain by combining bi-temporal ALS data and environmental data. For. Ecol. Manage. **481**: 118690. doi:10.1016/j.foreco.2020.118690

Hopkinson, C., Chasmer, L., and Hall, R.J. 2008. The uncertainty in conifer plantation growth prediction from multi-temporal lidar datasets. Remote Sens. Environ. **112**(3): 1168–1180. doi:10.1016/j.rse.2007.07.020.

Hudak, A.T., Strand, E.K., Vierling, L.A., Byrne, J.C., Eitel, J.U.H., Martinuzzi, S., and Falkowski, M.J. 2012. Quantifying aboveground forest carbon pools and fluxes from repeat LiDAR surveys. Remote Sens. Environ. **123**: 25–40. doi:10.1016/j.rse.2012.02.023.

Hunter, M.O., Keller, M., Victoria, D., and Morton, D.C. 2013. Tree height and tropical forest biomass estimation. Biogeosciences, **10**(12): 8385–8399. doi:10.5194/bg-10-8385-2013.

Isenburg, M. 2021. LAStools. Available from https://rapidlasso.com/ [accessed September 2021].

Jakubowski, M.K., Guo, Q., and Kelly, M. 2013. Tradeoffs between lidar pulse density and forest measurement accuracy. Remote Sens. Environ. **130**: 245–253. doi:10.1016/J.RSE.2012.11.024.

Jurjević, L., Liang, X., Gašparović, M., and Balenović, I. 2020. Is field-measured tree height as reliable as believed – part II, a comparison study of tree height estimates from conventional field measurement and low-cost close-range remote sensing in a deciduous forest. ISPRS J. Photogramm. Remote Sens. **169**: 227–241. Elsevier B.V. doi:10.1016/J.ISPRSJPRS.2020.09.014.

Knapp, N., Huth, A., Kugler, F., Papathanassiou, K., Condit, R., Hubbell, S.P., and Fischer, R. 2018. Model-assisted estimation of tropical forest biomass change: a comparison of approaches. Remote Sens. **10**(5): 1–23. doi:10.3390/rs10050731.

Lamb, S.M., MacLean, D.A., Hennigar, C.R., and Pitt, D.G. 2018. Forecasting forest inventory using imputed tree lists for LiDAR grid cells and a tree-list growth model. Forests, **9**(4): 1–18. doi:10.3390/f9040167.

Lee, C.C., and Wang, C.K. 2018. Effect of flying altitude and pulse repetition frequency on laser scanner penetration rate for digital elevation model generation in a tropical forest. GIScience Remote Sens. **55**(6): 817–838. doi:10.1080/15481603.2018.1457131.

Luoma, V., Saarinen, N., Wulder, M.A., White, J.C., Vastaranta, M., Holopainen, M., and Hyyppä, J. 2017. Assessing precision in conventional field measurements of individual tree attributes. Forests, **8**(2): 1–16. doi:10.3390/f8020038.

Magnussen, S. 1999. Effect of plot size on estimates of top height in Douglas-fir. West. J. Appl. For. **14**(1): 17–27. doi:10.1093/wjaf/14.1.17.

Magnussen, S., Næsset, E., and Gobakken, T. 2015. Lidar-supported estimation of change in forest biomass with time-invariant regression models. Can. J. For. Res. **45**(11): 1514–1523. doi:10.1139/cjfr-2015-0084.

Mauro, F., Ritchie, M., Wing, B., Frank, B., Monleon, V., Temesgen, H., and Hudak, A.T. 2019. Estimation of changes of forest structural attributes at three different spatial aggregation levels in northern California using multitemporal LiDAR. Remote Sens. **11**(8): 980. doi:10.3390/rs11080960.

McRoberts, R.E., Bollandsås, O.M., and Næsset, E. 2014. Modeling and estimating change. *In* Forestry applications of airborne laser scanning. Springer, Dordrecht, the Netherlands. pp. 293–313. doi:10.1007/978-94-017-8663-8_15.

McRoberts, R.E., Næsset, E., Gobakken, T., and Bollandsås, O.M. 2015. Indirect and direct estimation of forest biomass change using forest inventory and airborne laser scanning data. Remote Sens. Environ. **164**: 36–42. 10.1016/j.rse.2015.02.018.

Næsset, E. 2009. Effects of different sensors, flying altitudes, and pulse repetition frequencies on forest canopy metrics and biophysical stand properties derived from small-footprint airborne laser data. Remote Sens. Environ. **113**(1): 148–159. doi:10.1016/j.rse.2008.09.001.

Næsset, E., and Gobakken, T. 2005. Estimating forest growth using canopy metrics derived from airborne laser scanner data. Remote Sens. Environ. **96**(3–4): 453–465. doi:10.1016/j.rse.2005.04.001.

Næsset, E., Bollandsås, O.M., Gobakken, T., Gregoire, T.G., and Ståhl, G. 2013. Model-assisted estimation of change in forest biomass over an 11year period in a sample survey supported by airborne lidar: a case study with post-stratification to provide "activity data." Remote Sens. Environ. **128**: 299–314. doi:10.1016/j.rse.2012.10.008.

Natural Resources Canada. 2006. Stakeholders consultation for the development of the Canadian Height Reference System Modernization Implementation Plan. Available from https://www.pxw1.snb.ca/snb7001/e/PDF/hm_e.pdf [accessed May 2022].

Natural Resources Canada. 2020. Height reference system modernization. Available from https://www.nrcan.gc.ca/sites/nrcan/files/files/pdf/Height_reference_system_modernization_(EN).pdf [accessed May 2022].

Noordermeer, L., Gobakken, T., Næsset, E., and Bollandsås, O.M. 2020. Predicting and mapping site index in operational forest inventories using bitemporal airborne laser scanner data. For. Ecol. Manage. **457**: 117768. doi:10.1016/j.foreco.2019.117768.

Økseter, R., Bollandsås, O.M., Gobakken, T., and Næsset, E. 2015. Modeling and predicting aboveground biomass change in young forest using multi-temporal airborne laser scanner data. Scand. J. For. Res. **30**(5): 458–469. doi:10.1080/02827581.2015.1024733.

Penner, M., and Pitt, D. 2019. The Ontario Growth and Yield Program status and needs – Report to the Forestry Futures Trust Committee. Forestry Future Trust Committee, Ontario, Canada.

Pinheiro, J., and Bates, D. 2000. Mixed-effects models in S and S-PLUS. Springer, New York. Available from http://books.google.com/books?hl=en&lr=&id=RFDe_BKxvRIC&oi=fnd&pg=PR7&dq=Mixed-effects+models+in+S+and+S-plus&ots=mNw_ACYZH6&sig=fLQFxKjTyxOOLU4ypFI_a3pE8mE[accessed 12 July 2012].

Place, I.C.M. 2002. 75 Years of research in the woods: A history of Petawawa Forest Experiment Station and Petawawa National Forestry Institute, 1918 to 1993. General Store Publishing House, Burnstown, Ontario.

Poudel, K.P., Flewelling, J.W., and Temesgen, H. 2018. Predicting volume and biomass change from multi-temporal lidar sampling and remeasured field inventory data in panther creek watershed, Oregon, U.S.A. Forests **9**(1): 28. doi:10.3390/f9010028.

Pretzsch, H. 2020a. The course of tree growth. Theory and reality. For. Ecol. Manage. **478**(August): 118508. Elsevier. doi:10.1016/j.foreco.2020.118508.

Pretzsch, H. 2020b. Density and growth of forest stands revisited. Effect of the temporal scale of observation, site quality, and thinning. For. Ecol. Manage. **460**: 117879. doi:10.1016/J.FORECO.2020.117879.

Pretzsch, H. 2022. Facilitation and competition reduction in tree species mixtures in central Europe: consequences for growth modeling and forest management. Ecol. Modell. **464**: 109812. Elsevier B.V. doi:10.1016/j.ecolmodel.2021.109812.

Roussel, J.R., Auty, D., Coops, N.C., Tompalski, P., Goodbody, T.R.H. Meador, A.S., et al. 2020. lidR: an R package for analysis of airborne laser scanning (ALS) data. Remote Sens. Environ. **251**: 112061. doi:10.1016/J.RSE.2020.112061.

Ruiz, L.A., Hermosilla, T., Mauro, F., and Godino, M. 2014. Analysis of the influence of plot size and LiDAR density on forest structure attribute estimates. Forests, **5**: 936–951. doi:10.3390/f5050936.

Russell, M.B., Weiskittel, A.R., and Kershaw, J.A. 2014. Comparing strategies for modeling individual-tree height and height-to-crown base increment in mixed-species Acadian forests of northeastern North America. Eur. J. For. Res. **133**(6): 1121–1135. doi:10.1007/s10342-014-0827-1.

Sharma, M., and Parton, J. 2007. Height-diameter equations for boreal tree species in Ontario using a mixed-effects modeling approach. For. Ecol. Manage. **249**(3): 187–198. doi:10.1016/j.foreco.2007.05.006.

Sharma, M., Parton, J., Woods, M., Newton, P., Penner, M. Wang, J., et al. 2008. Ontario's forest growth and yield modelling program: advances resulting from the forestry research partnership. For. Chron. **84**(5): 694–703. doi:10.5558/tfc84694-5.

Skowronski, N.S., Clark, K.L., Gallagher, M., Birdsey, R.A., and Hom, J.L. 2014. Airborne laser scanner-assisted estimation of aboveground biomass change in a temperate oak-pine forest. Remote Sens. Environ. **151**: 166–174. Elsevier Inc. doi:10.1016/j.rse.2013.12.015.

Smith, D. 2018. The 2022 modernization of the national spatial reference system. Photogrammetric Engineering & Remote Sensing. **84**(6):337–338. doi:10.14358/PERS.84.6.337.

Socha, J., Pierzchalski, M., Bałazy, R., and Ciesielski, M. 2017. Modelling top height growth and site index using repeated laser scanning data. For. Ecol. Manage. **406**: 307–317. doi:10.1016/j.foreco.2017.09.039.

Stereńczak, K., Mielcarek, M., Wertz, B., Bronisz, K., Zajączkowski, G. Jagodziński, A.M., et al. 2019. Factors influencing the accuracy of ground-based tree-height measurements for major European tree species. J. Environ. Manage. **231**: 1284–1292. doi:10.1016/j.jenvman.2018.09.100.

St-Onge, B., and Vepakomma, U. 2004. Assessing forest gap dynamics and growth using multi-temporal laser-scanner data. Int. Arch. Photogramm. Remote Sens. Spat. Inf. Sci. **140**: 173–178.

Tompalski, P., Coops, N.C., White, J.C., and Wulder, M.A. 2014. Simulating the impacts of error in species and height upon tree volume derived from airborne laser scanning data. For. Ecol. Manage. **327**: 167–177. doi:10.1016/j.foreco.2014.05.011.

Tompalski, P., Coops, N.C., White, J.C., Wulder, M.A., and Pickell, P.D. 2015. Estimating forest site productivity using airborne laser scanning data and Landsat time series. Can. J. Remote Sens. **41**(3): 232–245. doi:10.1080/07038992.2015.1068686.

Tompalski, P., Coops, N.C., Marshall, P.L., White, J.C., Wulder, M.A., and Bailey, T. 2018. Combining multi-date airborne laser scanning and digital aerial photogrammetric data for forest growth and yield modelling. Remote Sens. **10**(2): 1–21. doi:10.3390/rs10020347.

Tompalski, P., Rakofsky, J., Coops, N.C., White, J.C., Graham, A.N.V., and Rosychuk, K. 2019. Challenges of multi-temporal and multi-sensor forest growth analyses in a highly disturbed boreal mixedwood forests. Remote Sens. **11**(18): 2102. doi:10.3390/rs11182102.

Tompalski, P., Coops, N.C., White, J.C., Goodbody, T.R.H., Hennigar, C.R. Wulder, M.A., et al. 2021. Estimating changes in forest attributes and enhancing growth projections: a review of existing approaches and future directions using airborne 3D point cloud data. Curr. For. Reports, **7**(1): 25–30. doi:10.1007/s40725-021-00139-6.

Treitz, P., Lim, K., Woods, M., Pitt, D., Nesbitt, D., and Etheridge, D. 2012. LiDAR sampling density for forest resource inventories in Ontario, Canada. Remote Sens. **4**(4): 830–848. doi:10.3390/rs4040830.

Tymińska-Czabańska, L., Socha, J., Hawryło, P., Bałazy, R., Ciesielski, M., Grabska-Szwagrzyk, E., and Netzel, P. 2021. Weather-sensitive height growth modelling of Norway spruce using repeated airborne laser scanning data. Agric. For. Meteorol. **308–309**: 108568. doi:10.1016/j.agrformet.2021.108568.

Van Laar, A., and Akça, A. 2007. Forest mensuration. Managing Forest Ecosystems. Springer, Dordrecht, the Netherlands.

van Lier, O.R., Luther, J.E., White, J.C., Fournier, R.A., and CôtCrossed D sign©, J.F. 2022. Effect of scan angle on ALS metrics and area-based predictions of forest attributes for balsam fir dominated stands. Forestry, **95**(1): 49–72. doi:10.1093/forestry/cpab029.

Véga, C., and St-Onge, B. 2008. Height growth reconstruction of a boreal forest canopy over a period of 58 years using a combination of photogrammetric and lidar models. Remote Sens. Environ. **112**(4): 1784–1794. doi:10.1016/j.rse.2007.09.002.

Wang, Y., Lehtomäki, M., Liang, X., Pyörälä, J., Kukko, A. Jaakkola, A., et al. 2019. Is field-measured tree height as reliable as believed – a comparison study of tree height estimates from field measurement, airborne laser scanning and terrestrial laser scanning in a boreal forest. ISPRS J. Photogramm. Remote Sens. **147**: 132–145. doi:10.1016/j.isprsjprs.2018.11.008.

Weiskittel, A.R., Hann, D.W., Kershaw, J.A., and Vanclay, J.K. 2011. Forest growth and yield modeling. John Wiley & Sons,Hoboken, NJ.

Wetzel, S., Swift, D.E., Burgess, D., and Robinson, C. 2011. Research in Canada's National Research Forests–past, present, and future. Forest Ecol. Manag **261**: 893–899. doi:10.1016/j.foreco. 2010.03.020

White, J.C., Wulder, M.A., Varhola, A., Vastaranta, M., Coops, N.C. Cook, B.D., et al. 2013. A best practices guide for generating forest inventory attributes from airborne laser scanning data using an area-based approach. Canadian Forest Service – Canadian Wood Fibre Centre, Information Report FI-X-10, Victoria, BC, Canada. doi:10.5558/tfc2013-132.

White, J.C., Coops, N.C., Wulder, M.A., Vastaranta, M., Hilker, T., and Tompalski, P. 2016. Remote sensing technologies for enhancing forest inventories: a review. Can. J. Remote Sens. **42**(5): 619–641. doi:10.1080/07038992.2016.1207484.

White, J.C., Tompalski, P., Vastaranta, M., Wulder, M.A., Stepper, C., Ninni, S., and Coops, N.C. 2017. A model development and application guide for generating an enhanced forest inventory using airborne laser scanning data and an area-based approach. Canadian Forest Service – Canadian Wood Fibre Centre, Victoria, BC, Canada.

White, J.C., Chen, H., Woods, M., Low, B., and Nasonova, S. 2019. The Petawawa research forest: establishment of a remote sensing supersite. For. Chron. **95**(3): 149–156. doi:10.5558/tfc2019-024.

White, J.C., Penner, M., and Woods, M. 2021a. Assessing single photon LiDAR for operational implementation of an enhanced forest inventory in diverse mixedwood forests. For. Chron. **97**(1): 78–96. doi:10.5558/tfc2021-009.

White, J.C., Woods, M., Krahn, T., Papasodoro, C., Bélanger, D., Onafrychuk, C., and Sinclair, I. 2021b. Evaluating the capacity of single photon lidar for terrain characterization under a range of forest conditions. Remote Sens. Environ. **252**: 112169. doi:10.1016/j.rse.2020.112169.

Wulder, M.A., Bater, C.W., Coops, N.C., Hilker, T., and White, J.C. 2008. The role of LiDAR in sustainable forest management. For. Chron. **84**(6): 807–826. doi:10.5558/tfc84807-6.

Yu, X., Hyyppä, J., Kaartinen, H., and Maltamo, M. 2004. Automatic detection of harvested trees and determination of forest growth using airborne laser scanning. Remote Sens. Environ. **90**(4): 451–462. doi:10.1016/j.rse.2004.02.001.

Zeide, B. 1993. Analysis of growth equations. For. Sci. **39**(3): 594–616.

Zhao, K., Suarez, J.C., Garcia, M., Hu, T., Wang, C., and Londo, A. 2018. Utility of multitemporal lidar for forest and carbon monitoring: tree growth, biomass dynamics, and carbon flux. Remote Sens. Environ. **204**: 883–897. doi:10.1016/j.rse.2017.09.007.

Zolkos, S.G., Goetz, S.J., and Dubayah, R. 2013. A meta-analysis of terrestrial aboveground biomass estimation using lidar remote sensing. Remote Sens. Environ. **128**: 289–298. doi:10.1016/j.rse.2012.10.017.